JOURNAL OF MATERIALS SCIENCE 26 (1991) 3497–3502

Synthesis of intermetallics for high temperature structural applications: $(Mn_5Si_3)16H$ crystal structure

P. B. CELIS, K. ISHIZAKI
Department of Materials Science and Engineering, School of Mechanical Engineering, Nagaoka University of Technology, Nagaoka, 940-21, Japan

The Zr–Si system was chosen to study the potentiality of the $(Mn_5Si_3)16H$ crystal structure for high temperature structural applications. A procedure was devised for the synthesis of intermetallics that have very high melting points. By hot isostatic pressing in a glass capsule, highly densified samples of Zr_5Si_3 were produced. Mechanical properties were measured. This compound is a good candidate for high temperature structural applications.

1. Introduction

In order to enhance the performance of heat engines, the temperature of the working fluid must be raised [1]. This temperature is limited by the maximum working temperature of the material used in these engines. The most widely used materials for high temperature structural applications are superalloys, which may perform at temperatures close to 1000 K. Silicon nitride is also being used in gas turbines at working temperatures close to 1300 K. However, materials for high temperature structural applications, which may withstand working temperatures as high as 1800 K, are desired [1]. These materials should be ductile and resistant to creep at those temperatures.

Recent discoveries suggest that among intermetallics, some compounds may offer these advantages. Positive temperature dependence of strength, has been confirmed in several intermetallics of the $(AuCu_3)4C$ crystal structure [2] as well as some other crystal structures [3]. Ductility has also been achieved in several intermetallic compounds by microalloying [4].

In this work the determination of intermetallic structures and intermetallic compounds for high temperature structural applications are explained. A procedure to synthesize highly densified samples of intermetallics by hot isostatic pressing (HIP) is outlined. Based on measurements of mechanical properties and X-ray diffraction analysis of the Zr_5Si_3 compound, the prospects of applications at high temperature are analysed.

Throughout this work, crystal structure is denominated according to the ASTM nomenclature, which is outlined elsewhere [5]. In Table I equivalent denominations of crystal structures which occur in the Zr–Si system are indicated.

2. Intermetallic compounds

Specific gravity (relative density) and melting point, as basic properties of any material, were used by Fleischer, to draw maps of intermetallic compounds [4]. Based on these maps, crystal structures are detected for high melting point with low specific gravity.

Creep resistant materials usually have a high melting point. On the other hand, low specific gravity is desired in the aircraft industry and in moving parts such as turbine blades. For practical purposes, specific gravity may be limited to that of superalloys [6].

2.1. Crystal structure

Compounds with the $(Mn_5Si_3)16H$ crystal structure have specific gravities in the range of 4 to 8, and some of them have melting points as high as 2800 K, indicating that they are candidates for high temperature structural applications.

Pettifor has devised crystal structure maps for intermetallic compounds [7, 8, 9]. Using these maps, it is possible to roughly predict which elements may form a certain crystal structure. Choosing appropriate elements, it is possible to engineer, to a certain degree, the basic properties such as melting point and specific gravity in crystal structures.

Equilibrium diagrams on alloy systems of high melting point are limited. The higher the melting point of a compound, the larger the error of values found in the literature. In the case of the (Mn_5Si_3) 16H crystal structure silicon compounds of a certain element tend to have higher melting points than germanium compounds, for 100–300 K. The melting point of a silicon compound could be estimated, providing that the melting point of the germanium compound is known. Among the germanium compounds with this crystal structure, Zr_5Ge_3 has one of the highest melting points [4]. Therefore, it may be expected that the Zr_5Si_3 compound will have a very high melting point of around 2600 K.

2.2. The Zr–Si system

In this work, the potential of the $(Mn_5Si_3)16H$ crystal structure for high temperature structural applications

0022–2461/91 $03.00 + .12

TABLE I Equivalent crystal structure nomenclatures for compounds of the Zr–Si system.

Compound	Type	ASTM Nomenclature	Strukturbericht Name	Pearson index
Zr	Mg	2H	A3	hP2
Zr_3Si	PTi_3	32T	–	tP32
Zr_2Si	Al_2Cu	12U	C16	tI12
Zr_5Si_3	Mn_5Si_3	16H	$D8_8$	hP16
Zr_3Si_2	U_3Si_2	10T	–	tP10
Zr_5Si_4	Zr_5Si_4	36T	–	tP36
ZrSi	BFe	80	B27	oP8
$ZrSi_2$	$ZrSi_2$	12S	C49	oC12
Si	C	8F	A4	cF8

is assessed, based on the Zr–Si system. The Bravais lattice of the $(Zr_5Si_3)16H$ is hexagonal with three different basal planes stacked in the following order: ABACA. Basal planes B and C have a similar atomic distribution, but are rotated 180° from each other, as shown in Fig. 1.

To understand better the particularities of the $(Zr_5Si_3)16H$ crystal structure, packing was studied comparing the different structures of the Zr–Si system. In Fig. 2a, the theoretical density of the different compounds is plotted as a function of the Zr atomic fraction. The linearly averaged density between Zr and Si is shown by the dashed line. In Fig. 2b, the excess density, i.e. the difference between the compounds' theoretical density and the linearly averaged value of Zr and Si, is also plotted against the Zr atomic fraction. This figure indicates the degree of packing of each structure. The (ZrSi)80 has the highest packing as should be expected. However, it is also interesting to note that the $(Zr_5Si_3)16H$ structure has a higher degree of packing than the $(Zr_3Si_2)10T$ structure, which has a closer stoichiometric ratio to that of the (ZrSi)80 compound.

Similarly, the nearest neighbour distance between Zr and Si atoms was plotted against the Zr atomic fraction, as shown in Fig. 3a. In Fig. 3b, the excess distance, i.e. the difference between each compound nearest neighbour distance and the linearly averaged nearest neighbour distance of Zr and Si is plotted against the Zr atomic fraction. The solid line in Fig. 3a and b has no physical meaning, and is only drawn for graphic clarity. In the case of the (ZrSi)80 compound, the value is slightly negative, indicating that the packing is not only affected by the size difference of the atoms, but is also affected by the bonding strength between Zr and Si atoms. However, it is the $(Zr_5Si_3)16H$ structure that has the most negative value, and the overall shortest nearest neighbour distance, thus indicating a very strong Zr–Si bonding. This bonding provides such a high melting point in this crystal structure.

3. Experimental procedure

The most widely used method to produce intermetallic compounds from the powder elements is the argon-arc method. In this method, a sample of adequate proportions of different elements is mixed in powder form. The sample is then placed on a cooled hearth

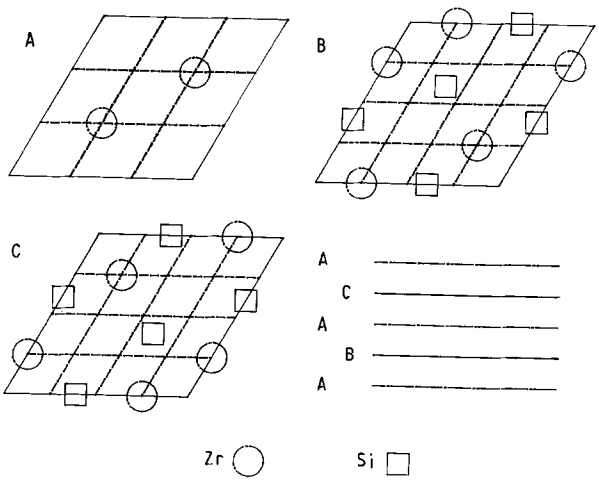

Figure 1 Three kinds of basal planes in the crystalline structure of the Zr_5Si_3 intermetallic compound. The stacking order of these planes is ABACA as shown in the figure.

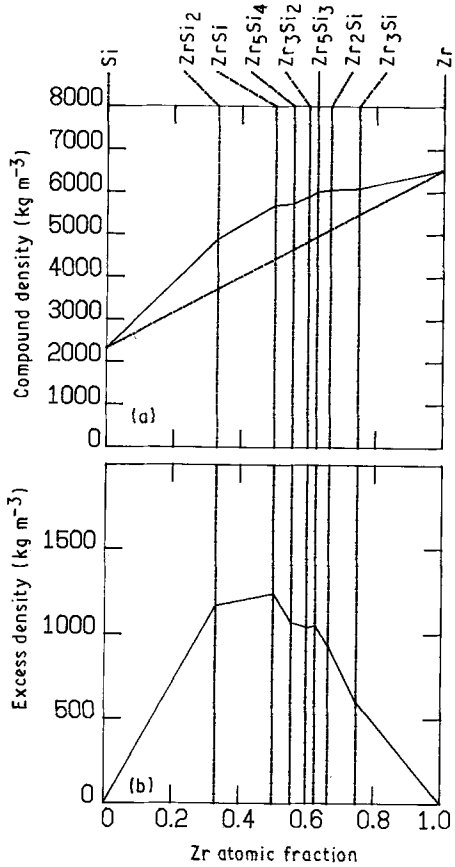

Figure 2 (a) Theoretical density in the solid line and linearly arranged density in the dashed line, and (b) excess density, i.e. theoretical density minus the linearly averaged Si–Zr density are plotted against Zr atomic fraction.

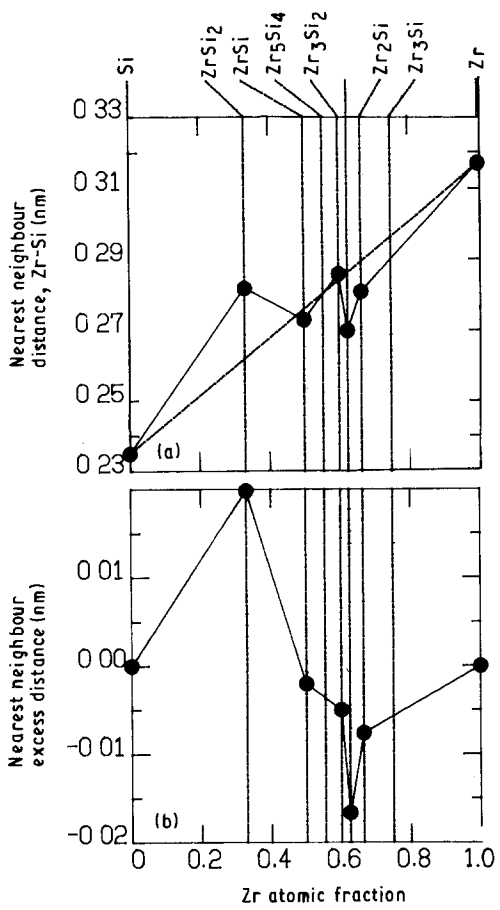

Figure 3 (a) Nearest neighbour distance in the solid line and linearly averaged nearest neighbour distance in the dashed line and (b) excess nearest neighbour distance are plotted against Zr atomic fraction. The solid line has no physical meaning, and it is only used for graphic clarity. The solid circles have the physical meanings.

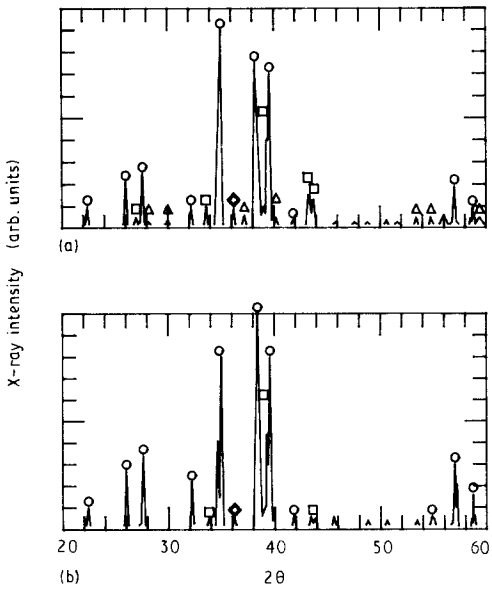

Figure 4 X-ray diffraction pattern of (a) sample in which reaction was triggered by an argon arc for 3–4 s and a current of 60 A, and (b) sample heated twice continuously by argon arc for 60 s and 150 A to melt completely. Key: (Δ) Zr_3Si_2, (○) Zr_5Si_3, (□) Zr_2Si and (◇) Zr.

and heated with an argon-arc plasma. This method has several disadvantages: 1. the high melting point compounds are sometimes not heated enough on a cooled plate; 2. the gas is usually trapped in the sample, thus producing a high porosity sample; 3. the cooling rate is extremely fast, thus creating thermal stresses and cracks in the sample; and 4. in the case of compounds in which elements have different vapour pressures or melting points, the low melting point element is lost during melting, thus alterating the stoichiometry of the sample.

3.1. Reaction between Zr and Si

In this work, the reaction of samples was triggered by an argon arc, but melting was avoided to prevent Si loss. The heat produced by the following reaction,

$$5Zr + 3Si \rightarrow Zr_5Si_3 \quad (1)$$

is enough to activate the same reaction in the vicinity, and is also enough to allow for a high degree of homogenization of the crystal structure in the sample.

The effect of melting may be understood through the X-ray diffraction patterns shown in Fig. 4. For the sample shown in Fig. 4a, the reaction was triggered by an argon arc for 3–4 s and a current of 60 A. This sample was deformed but not melted. The sample of Fig. 4b was heated continuously by the argon arc for 60 s and a current of 150 A until melted. To avoid heterogeneity, the sample was turned over on the copper hearth, then the same amount of heat was applied by the argon arc on the opposite surface. In this case, the shape of the sample was completely changed into a liquid droplet. The X-ray pattern of the melted sample, as shown in Fig. 4b, indicates that there is no silicon rich Zr_3Si_2 phase. Demonstrating therefore, that there is silicon loss during melting.

3.2. Densified Zr_5Si_3 samples

Highly densified samples of Zr_5Si_3 were produced according to the flow chart of Fig. 5. Stoichiometric amounts of Zr and Si to synthesize Zr_5Si_3 were mixed in a ball mill equipment with ethanol. After drying in vacuum, powders were cold isostatic pressed (CIP) into cylinders at 400 MPa. These samples were triggered to react in an argon arc, avoiding the melting. Samples were crushed by a mortar until the powder passed through a No. 150 mesh. An X-ray diffraction pattern was taken for phase analysis. Finally, these powders were once again subjected to CIP at 400 MPa and made into cylinders 12 mm dia. and 15 mm long.

Densification of high melting point substances requires sintering at very high temperatures. Reaction between the intermetallic compound and the glass capsule used during the HIP process was successfully avoided by applying a thick layer of boron nitride powder. To apply this layer (~ 1 mm thick) samples were once again subjected to CIP at 400 MPa.

Samples were degassed at 1273 K and 1 Pa for 1 h and capsuled in vycor glass. These capsules were HIP'ed for 1 h. at 1973 K and 2273 K under 100 MPa. A typical HIP sintering cycle for glass capsules is shown in Fig. 6.

After Archimedian density measurements in water the samples were cut and crushed to take the X-ray diffraction pattern, or polished to measure mechanical properties.

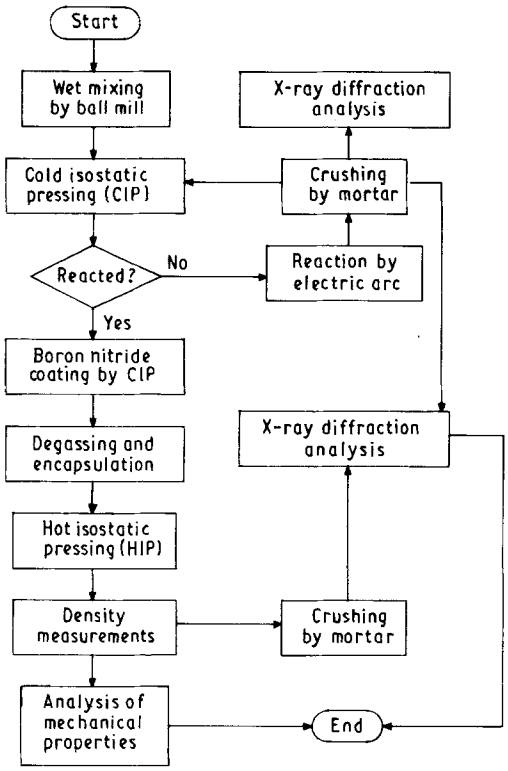

Figure 5 Flow chart of the experimental synthesis of the Zr_5Si_3 intermetallic compound.

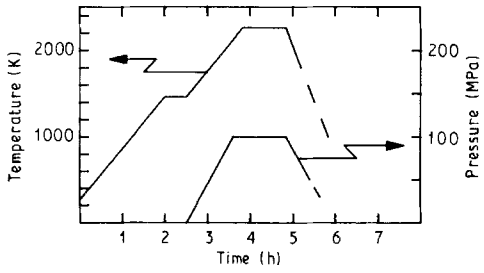

Figure 6 Typical HIP'ing cycle for glass capsules.

Elastic constants were determined by sound velocity measurements. Hardness and fracture toughness were measured by Vickers indentation tests. Hardness measurements were made applying a 0.5 kg load to a diamond indenter. Cracks were produced in the samples when a 5 kg load was applied, and used to calculate fracture toughness. The distance from the centre of the indentation to the tip of the crack (a) is introduced in the following equation to obtain an estimate of the fracture toughness:

$$K_{IC} = 0.0725L/a^{3/2} \quad (2)$$

where L is the load applied during the indentation test [10].

3.3. Materials

Two types of Zr powders were used to study the grain size effect in the Zr–Si reaction. The main characteristics of these powders and the silicon powder are shown in Table II.

4. Results and discussion

X-ray diffraction patterns of powdered samples are shown for the not-melted samples in Fig. 7, and the HIP'ed samples in Figs 8 and 9. A comparison of properties of HIP'ed Zr_5Si_3 samples with other engineering materials is found in Table III.

4.1. Synthesis of Zr_5Si_3

The synthesis of this material may be divided in two stages: the reaction stage, and the sintering stage. They will be treated separately in this section.

4.1.1. Reaction stage

Different stoichiometric mixtures of Zr–Si were made, using only Zr powder A, 50% of Zr powder A plus 50% of Zr powder B, and only Zr powder B. X-ray diffraction patterns of the reacted powders are shown in Fig. 7. Notice how the phase distribution changes for each powder mixture. A greater average diameter of powder A resulted in a purer Zr_5Si_3 phase. During the experiment samples of powder B, with a smaller average particle diameter, tended to explode into several pieces due to the violent reaction. However, samples of powder A were only deformed when the intense heat of the reaction was released. This indicates that the purity of the reacted phase can be controlled by the reaction rate, which can be governed by particle size of the starting powders, as shown here, or by mixing reacted powders with the unreacted ones in proper quantities to obtain the desired reaction rate.

4.1.2. Sintering stage

A type B Zr powder was used in preparing Zr_5Si_3 powders for HIP'ing. Therefore, purity of Zr_5Si_3 in the starting powders was low due to the violent reaction as already explained. It was expected that homogenization of the sample could be achieved during the HIP'ing treatment. However, even at a sintering temperature of 2273 K, phase homogenization could not be achieved. This indicates the necessity of even higher temperatures for HIP'ing or controlling the phase purity of the starting powders, so that a high purity and fully densified sample may be produced by

TABLE II Raw material characteristics

Element	Label	Purity	Average dia. (μm)	Mesh no.
Zr	A	98%	5	–
Zr	B	98.5% (Zr + Hf)	3.5	–
Si	C	99.5%	–	350

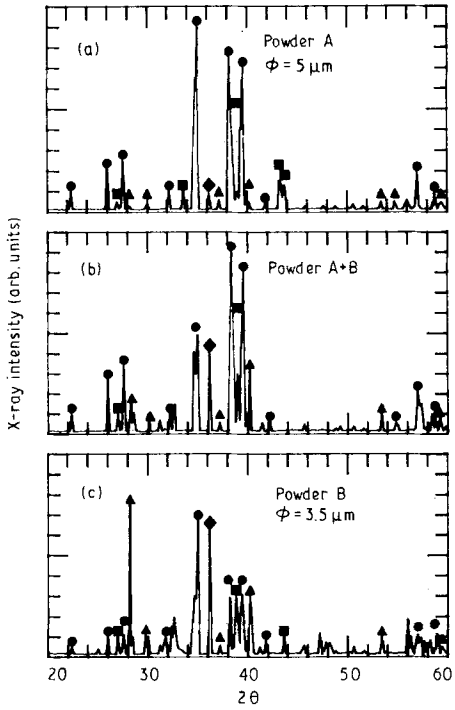

Figure 7 X-ray diffraction patterns of reacted Si–Zr powder mixtures: (a) Zr powder A, (b) 50% Zr powder A and 50% Zr powder B and (c) Zr powder B. Key: (▲) Zr_3Si_2, (●) Zr_5Si_3, (■) Zr_2Si, and (◆) Zr.

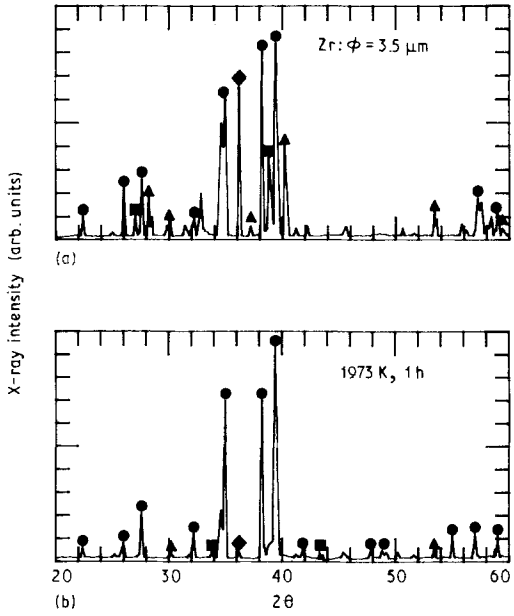

Figure 8 X-ray diffraction pattern for Zr_5Si_3 samples (a) before and (b) after being HIP'ed at 1973 K for 1 h. Key: as for Fig. 7.

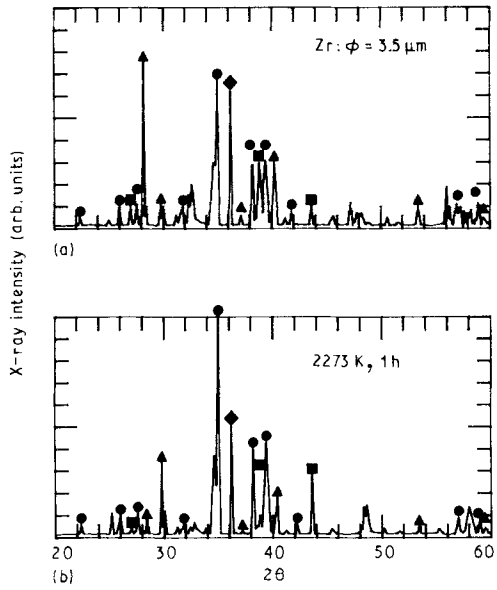

Figure 9 X-ray diffraction pattern for Zr_5Si_3 samples (a) before and (b) after being HIP'ed at 2273 K for 1 h. Key: as for Fig. 7.

HIP treatment. On the other hand, this also indicates that diffusion mechanisms are very slow inside this material even at 2273 K. From this result, it can be infered that this material should have good creep resistance at high temperatures.

X-ray diffraction patterns of samples from the smaller raw powder B HIP'ed at 1973 K and 2273 K for 1 h are shown in Figs 8 and 9, respectively. Because of the violent reaction of the powder B, the reproducibility of the product was not good. High temperature HIP sintering was employed to obtain homogeneous Zr_5Si_3. The material is shown before and after HIP sintering in Figures (a) and (b), respectively. Comparing Figs 8a and 9a it can be seen that starting powders for the HIP treatment at 1973 K are purer than for the HIP treatment at 2273 K. Therefore, a purer sample was obtained even though the sintering temperature was low. However, samples sintered at 2273 K had a very high relative density (97%), while samples sintered at 1973 K achieved only 95% of relative density.

4.2. Mechanical properties of Zr_5Si_3

Values of mechanical properties for Si_3N_4· Zr_5Si_3 · IN-939 superalloy and Ni_3Al are shown in Table III. Si_3N_4 values were taken from several references [11, 12, 13]. Zr_5Si_3 values were measured in this work. Melting temperature is a conservative approximation. Elastic constants were calculated from sound velocity measurements, and hardness and fracture toughness were determined from Vikers indentation tests in the most densified samples (97% of relative density). Elastic constants of superalloy [14] and Ni_3Al [15, 16] are also tabulated here.

Elastic constants in Zr_5Si_3 are higher than in superalloys but lower than in ceramics such as Si_3N_4. These values give an idea of the nature of the Zr–Si bonding. The bonding is not as stiff as the covalent bonding of Si–N, but stiffer than metallic bondings of superalloys. So that these Zr–Si bondings may be described as metallic and covalent bondings.

Hardness is also a measure that describes bonding strength as well as plasticity of a material. Therefore, a lower value than that of Si_3N_4 is expected for Zr_5Si_3. Fracture toughness was expected to have a higher value than for Si_3N_4, however, it is slightly lower, thus indicating brittleness in this material. Nevertheless, there is room for improvement as this material was not yet fully densified.

TABLE III Mechanical properties at room temperature for several different materials. Values for the Zr_5Si_3 intermetallic compound were measured in this work

Properties	Compound			
	Si_3N_4	Zr_5Si_3	IN-939	Ni_3Al
Physical properties				
Melting point (K)	2200 (de.)	2600	1508	1668
Theoretical density (kg m^{-3})	3180	5998	8160	7469
Elastic properties				
Sound velocity ($ms^{-1}/8$) – longitudinal	10565	6770	5880	5690
– transversal	6220	3860	3050	3030
Elastic modulus (GPa)	304	220	200	179
Shear modulus (GPa)	123	87	76	69
Poisson's ratio	0.24	0.26	0.31	0.30
Bulk modulus (GPa)	191	152	181	150
Debye temperature (K)	1100	480	450?	450
Other mechanical properties				
Vickers hardness (GPa)	$16.0^{+1.5}_{-1.5}$	$11.9^{+1.0}_{-1.1}$	–	–
Fracture toughness ($MNm^{-3/2}$)	$5.5^{+0.5}_{-0.5}$	$3.5^{+1.2}_{-0.7}$	–	–

5. Conclusions

The Zr_5Si_3 material was synthesized in powder and in bulk form. From the results obtained, the following points are concluded:

(a) Compounds that have the (Mn_5Si_3) 16H crystal structure have specific gravities lower or equal to those of superalloys. Some compounds of this structure exhibit extremely high melting points, that make them excellent candidates for high temperature structural applications. Specifically, the Zr_5Si_3 intermetallic compound has the lowest nearest neighbour distance of the compounds present in the Zr–Si system, thus indicating that this (Zr_5Si_3)16H crystal structure has particularly strong Zr–Si bonding.

(b) When synthesizing Zr_5Si_3, close control of reaction rate allows to control the phase purity of the compound. Melting should be avoided to prevent Si loss when Zr and Si powders are reacting.

(c) The low speed of diffusion mechanisms prevents a quick homogenization and densification of the material during HIP'ing. Purer starting powders should be used, as well as longer holding time or higher sintering temperature during HIP'ing.

(d) Elastic constants and hardness values reflect the metallic and covalent nature of the Zr–Si bonding in the Zr_5Si_3 compound. Fracture toughness indicates that Zr_5Si_3 is a brittle material, however, this value may be improved by fully densifying the material.

(e) Low diffusivity at high temperatures, a strong bonding between the elements, and high stiffness as well as hardness values indicate that the Zr_5Si_3 intermetallic compound is a good candidate for high temperature structural applications. Nevertheless, further research is necessary to fully assess its high temperature structural capabilities.

Acknowledgements

This research was partially supported by a cooperative program of the Ministry of Education and Culture (MONBUSHO) and Kobe Steel Co. HIP treatment at 2273 K was kindly provided by Kobe Steel Co. The sharing time of the X-ray diffractometer was supplied by the Analysis Center of the Nagaoka University of Technology.

References

1. A. I. TAUB and R. L. FLEISCHER, *Science* **243** (1989) 616.
2. ASTM Nomenclature Subcommittee of Committee E-4 on Metallography, *ASTM Bulletin* Dec. (1957) 27, (TP215).
3. D. M. WEE, O. NOGUCHI, O. YOSHIHIRO and T. SUZUKI, *Trans. Jpn Inst. Met.* **21** (1980) 237.
4. R. L. FLEISCHER, *J. Mater. Sci.* **22** (1987) 2281.
5. K. AOKI and O. IZUMI, *Jpn. Inst. Met.* **43** (1979) 1190.
6. D. L. ANTON, D. M. SHAH, D. N. DUHL and A. F. GIAMEI, *J. Met.* Sept. (1989) 12.
7. D. G. PETTIFOR, *Solid State Communications* **54** (1984) 31.
8. *Idem, Solid State Physics* **19** (1986) 285.
9. *Idem, Mater. Sci. Technol.* **4** (1988) 675.
10. K. TANAKA, *J. Jpn. Inst. Met.* **48** (1984) 1157.
11. D. W. RICHERSON, (ed.) "Modern Ceramics Engineering-Properties, Processing and Use in Design", (Marcel Dekker, New York, 1982).
12. K. WATARI, Y. SEKI and K. ISHIZAKI, *J. Ceram. Soc. Jpn. (Internat. Ed.)* **97** (1989) 170.
13. T. HAMASAKI, K. ISHIZAKI and K. TANAKA, *ibid.* **98** (1990) 995.
14. "Metals Handbook", 9th edition, Vol. 3, (American Society for Metals, 1985) p. 242.
15. K. ONO and R. STERN, *Trans. Metall. Soc. AIME* **245** (1969) 171.
16. K. ISHIZAKI and P. B. CELIS, 'Ultra High Temperature Resistant Materials and Intermetallics', in "Handbook of New Materials", vol. 6, "Metallic Materials", edited by Kasuhiro Goto (Kabushiki Gaisha Shokodo, Tokyo, 1990), in press.

Received 2 May 1990
and accepted 29 October 1990